

# Always aim high

## EWEA 2015 Annual Event



**EWEA 2015**  
PARIS  
EUROPE'S PREMIER WIND ENERGY EVENT

## Scientific Proceedings

EWEA Annual Conference and Exhibition  
Paris, France

IN PARTNERSHIP AND SUPPORTED BY:



ORGANISED BY:



**EWEA**  
THE EUROPEAN WIND ENERGY ASSOCIATION



**EWEA 2015**  
P A R I S  
EUROPE'S PREMIER WIND ENERGY EVENT

# Scientific Proceedings

**Publisher:**

European Wind Energy Association (EWEA)

**Responsible:**

Alice Rosmi

Rue d'Arlon 80, B-1040 Brussels, Belgium

Tel: +32 2 213 1811 Email: [ewea@ewea.org](mailto:ewea@ewea.org)

**Printed by:**

Artoos



# Alternative Wind Turbine Drive Train with Power Split and High-speed Generators

Cristian Andrei<sup>1</sup>

Simon Serowy<sup>2</sup>

Friederike Barenhorst<sup>2</sup>

Björn Riemer<sup>1</sup>

Ralf Schelenz<sup>2</sup>

Kay Hameyer<sup>1</sup>

<sup>1</sup>Institute of Electrical Machines (IEM), RWTH Aachen University  
Schinkelstraße 4, 52062 Aachen, Germany

<sup>2</sup>Institute for Machine Elements and Machine Design (IME), RWTH Aachen University  
Schinkelstraße 10, 52062 Aachen, Germany

## 1. Abstract

Conventional wind turbines (WTs) have large weight and size, reliability issues and show potential for efficiency increase at partial load. This paper describes an alternative 6 MW WT drive train, which uses the power split concept to enable its high-speed generators to operate in their optimal operating point. A design with more carry-over parts is possible, which reduces maintenance time and leads to an efficient manufacturing process. The system is also redundant when individual drive trains fail. Different gearbox configurations and generator topologies are evaluated for the proposed concept and an operating strategy is developed.

## 2. Keywords

Wind power generation, wind turbine drive train, power split gearbox, permanent magnet synchronous machine, high-speed generator.

## 3. Wind Turbine Concepts

Today's wind energy market displays a variety of drive train topologies with different generator concepts, which impose different challenges on the gearboxes and power converters [1].

Direct driven WT's are designed with no gearbox, which results in low speeds and high torques at the generator. The generators are commonly synchronous machines with high pole pair numbers. Their excitation is realized on the rotor with an electrical winding or with permanent magnets. These generators are large, heavy, challenging to transport and require a high amount of copper for the windings. In case of permanent magnet excitation, rare earth magnets are required, which represent a financial insecurity, due to the price fluctuations over the last years [2].

Further established WT concepts are based on medium-speed (100 – 400 rpm) or high-speed (up to 2,000 rpm) generators. Medium-speed generators are also synchronous machines (most common with permanent magnets). Usually they are integrated with an one- or a

two-stage gearbox. This results in a more compact construction compared to direct driven generators [3]. However, higher maintenance and an increased cost factor, due to the design with gearbox and the use of permanent magnets, are still an issue. Both direct driven and medium-speed generators require a full power converter for the adjustment of the grid frequency, due to dynamic operation with fluctuating wind conditions. This adds to the overall costs, because of the relatively high prices of the power electronics components.

WTs with high-speed generators mostly use doubly-fed induction machines combined with a three-stage gearbox. For this concept the stator is directly coupled to the grid and the frequency adjustment is realized by a converter in the rotor winding system. Disadvantages of this concept are the reduced speed variability and the fault-prone gearbox. Being a mature technology, this is nevertheless the most cost-effective concept on the market.

Additional alternative concepts have also been developed. Clipper's Liberty is a 2.5 MW WT with a similar construction to the concept proposed in this paper [4]. The gearbox consists of two spur gear stages and the power is split between four permanent magnet synchronous generators, which rotate at 1,133 rpm. For the individual drive trains, the power is split and then summated in the gearbox from two different power paths. This mechanical redundancy has led to significant issues in the gearbox.

Another WT gearbox configuration with power split is the Multi Duored concept from Winergy [5]. This gearbox uses spur gear stages for an eight-fold power split with subsequent four-fold power summation, leading to only two outputs. The combination of power split and power summation and the exclusive use of spur gears yields a high number of carry-over parts, but also leads to a large weight (62 t for 6.5 MW).

Today's available WT concepts do not take full advantage of the modularity and redundancy of

a drive train with power split, or the material and cost reduction of high-speed electrical machines. In order to achieve these goals, an alternative drive train is proposed and its development is described in the following sections. The potential of an efficiency increase over a wide operating range at partial load (especially below 30 % rated power) is shown, where typical efficiencies of conventional WT's drop significantly to under 80 %, irrespective of the used concept [6], [7].

## 4. Proposed Drive Train

Figure 1 illustrates the concept of the 6 MW WT drive train with six 1 MW high-speed (5,000 rpm) generators and a four-stage gearbox with power split. The gearbox in Figure 1 consists of one spur and three planetary gear stages and realizes the power split in the first stage. The generator is designed as a permanent magnet synchronous machine (PMSM). These gearbox and generator topologies are described in sections 5 and 6, alongside other configurations that were also considered in the development process.

The gearbox used for this concept needs a higher transmission ratio compared to conventional configurations. Higher losses due to the higher transmission ratio can be compensated by an optimized operating strategy and the benefits of the high-speed machines. The targeted higher speed results in an increased power density, which leads to a considerable reduction of weight and size of the generators. Furthermore this reduces the amount of active magnetic material and decreases investment costs. The design with multiple identical generators enables the utilization of more carry-over parts. These parts are at the same time smaller and more lightweight due to the power split configuration. As a result increased economic efficiency in

production and improvements in maintenance can be achieved. Mechanical power split with subsequent electrical power summation on the grid side is also a more robust solution, than a purely mechanical split and summation of the power inside the gearbox. A certain redundancy of the system is given as well, since energy will still be produced, even when one or more generators fail.

## 5. Gearbox Configurations

The predesigned gearbox concepts for the high-speed multi-generator drive train are basically similar to the structure of conventional WT gearboxes. They are built as a combination of planetary and spur gear stages. The planetary stages are considered exclusively in the two-shaft mode (drive: planet carrier, driven: sun shaft) in order to restrict the solution space. With the use of planetary gears a compact space with high power density and high transmission ratios can be obtained. To implement the power split to six generators, a spur gear is used. Since the intended rated speed of the generators is 5,000 rpm, the gearbox needs to have a transmission ratio higher than 1:400. To realize this ratio, only gearbox concepts with four gear stages are considered. In order to develop a modular configuration, the gearbox concepts consist of standard and independent gear stages, joined together through couplings. In case of a malfunction the faulty gearbox component can thus be completely replaced and the downtime of the WT can be reduced.

Different gearbox concepts have been developed and evaluated in order to determine the best solution for this drive train concept. In a multi-level rating scheme there have been four concepts identified for the further examination. Depending on the requirements for space and durability, shafts, bearings and gears are dimensioned based on the rated load

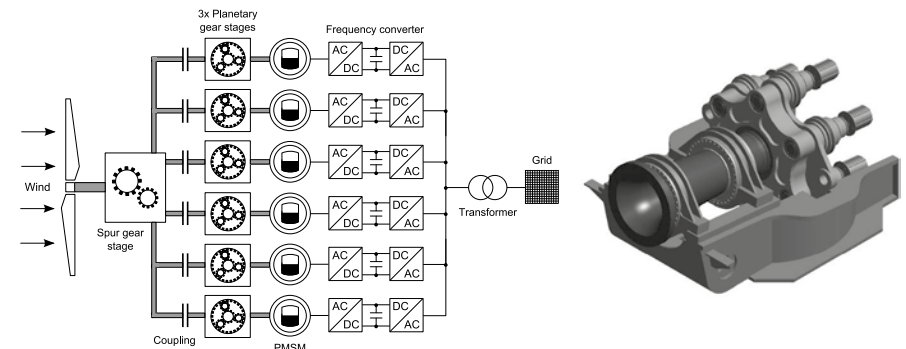


Figure 1: Concept and CAD model of the proposed alternative WT drive train.

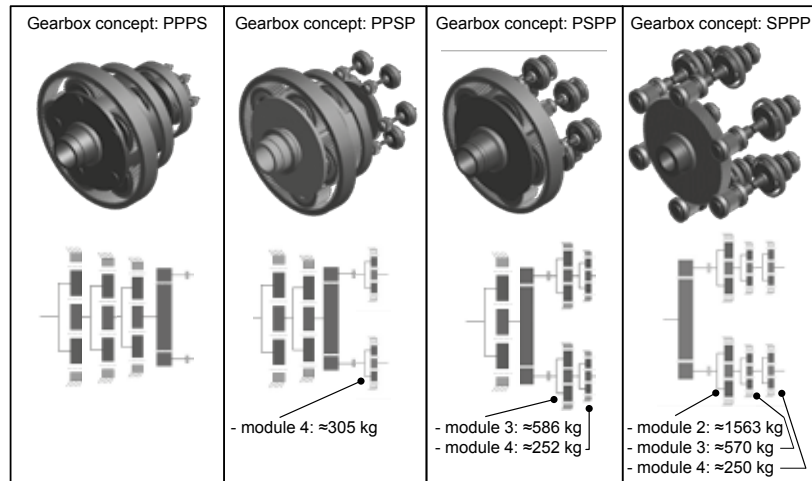


Figure 2: Studied gearbox concepts.

Gearbox concept	PPPS	PPSP	PSPP	SPPP
Weight (Gears, shaft, bearings)	≈ 47 t	≈ 49 t	≈ 45 t	≈ 40 t
Size (Width × length)	3.4 × 3.4 m	3.4 × 3.4 m	3.4 × 3.2 m	4.2 × 3 m
Total number of parts	90	193	275	370
Number of different parts	28	31	30	31
Modularity	3.21	6.23	9.17	11.94

Table 1: Comparison of different gearbox concepts.

for these four gearbox concepts (see Figure 2). The four gearbox configurations in Figure 2 consist of three planetary stages (P) and a spur gear stage (S). The concepts differ in the position of the spur gear stage and thus the power split in the gearbox.

A challenge of these gearbox concepts is the shaft bearing for the spur gear used to realize the power split. Switchable couplings are designated behind the power split, which are opened or closed depending on the input power. The generators are ramped up to the synchronous speed before the couplings are activated, which reduces the wear. Positive fit and frictionally engaged couplings, both dry- and wet-running, are evaluated for this application. While a coupling is opened the associated spur gear output shaft is rotating anyway, because the gearing is still in operation. Though the shaft is not transmitting power – other than the friction in the bearings – the tooth forces in this operational state are quite low. The bearings are pre-stressed with an initial tension, in order to reduce the operating risk of the bearings below minimum load. This initial tension is 2 % of the load rating for the used tapered roller bearings [8].

The developed concepts are rated regarding space, weight, modularity and efficiency. To give a statement on the modularity of the different concepts, a parameter is introduced that rates the total number of identical parts to the number of different parts. The result is the average number of used elements in the entire gearbox. The higher this parameter is, the higher is the modularity of the concept. Only the parts from the bottom level of the bill of materials are considered to be single parts. Only shafts, bearings, planet carrier and gears are regarded.

In Table 1 the four gearbox concepts are compared. The use of planetary gear units in the first three stages leads to a compact gear design with a low modularity. The concept with power split in the first stage stands in direct contrast to this structure. For this concept six individual 1 MW gear trains, each with three planetary stages, are arranged after the first stage. This leads to a very modular gearbox structure, increases the number of identical parts and reduces the mass of the individual components. The remaining concepts provide the power split in the second and third stage, respectively.

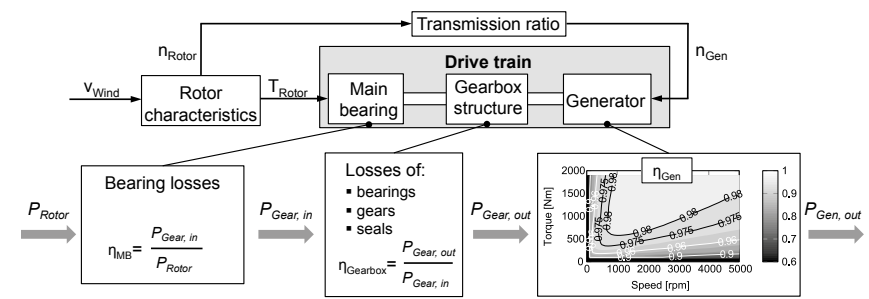


Figure 3: Structure of the efficiency calculation model.

The comparison of the four gearbox concepts regarding their efficiency is carried out on a system level. In order to perform efficiency calculations for the entire drive train – including main bearing, gearbox with six-fold power split and generators – an AMESim model of the entire system is created (see Figure 3). The main bearing is designed as a fixed-floating bearing system, as it is typically used in WT drive trains with four point suspension. For the developed gearbox structures, the used seals, bearings and gear parameters are implemented in the model. The generators are modeled based on the efficiency map of the PMSM described in section 6.

To calculate the efficiency the power losses of every component are determined for all operating points of the gearbox based on analytic equations. These power losses are – regarding the bearings and gears – both load-dependent and -independent. The bearing losses are calculated for the main bearing and other bearings used in the gearbox, according to established calculation methods [8].

There are commonly hydrodynamic and friction losses occurring in the tooth contact. In the used calculation model these friction losses are divided into rolling and sliding friction and calculated for every tooth engagement [9]. The hydrodynamic losses are divided into churning and squeezing losses. These losses cannot be calculated in AMESim using the underlying empiric equations by Terekhov [10]. Terekhov's calculation method is based on research on spur gears with a maximum module of 8 mm, which are evaluated at maximum circumferential speeds of 50 m/s [11]. However, the developed gearbox concepts use big teeth with modules of 10-24 mm, in the gear stages before the power split. Moreover, the circumferential speed in the PPS gearbox concept is higher than 50 m/s in the fourth stage which means that Terekhov's methods lose their validity. According to Strasser, the load-independent losses (churning and squeezing

losses) represent 1-13 % of the entire losses in the gearbox, depending on the operating point [11]. As long as there is an oil injection lubrication instead of a flood lubrication for every stage, no churning losses occur. The squeezing losses can be estimated at 0.37-10 % [11]. The relative comparability of the gearbox concepts based on their efficiency is still given, because the operating points of every concept are identical and due to the fact that the squeezing losses depend mainly on the circumferential speed and the lubricant viscosity [12]. For the seals, load independent losses are calculated using the approach according to [13].

The efficiency is defined as the relation of the generator output power and the rotor input power. First simulations are carried out at a lubricant temperature of 65 °C and for a start-up procedure of the WT up to rated power. No operating strategy regarding power split is implemented at this point, which means that all generators are symmetrically loaded at partial load. Figure 4 depicts the efficiencies of four different drive train configurations, where only the gearbox concept varies.

The variation during the entire operating range between the different concepts is less than 1 %, which is within the accuracy of the model. The drive train concept with power split in the third stage (PPSP) exhibits the best efficiency with 93.7 % at full load. The concepts with power split in the first (SPPP) and last stage (PPPS) basically display identical efficiency curves with a maximum efficiency of about 93.5 % at full load. The concept with power split in the second stage (PSPP) has 0.25 % lower efficiency.

The anticipated result, that the gearbox concept with the highest number of rotating parts (SPPP) would show the worst and the concept with the smallest number of parts (PPPS) the best efficiency, has not been confirmed. This can be traced back to the use of different roller bearings and the slightly different transmission ratio of the different concepts, due to their

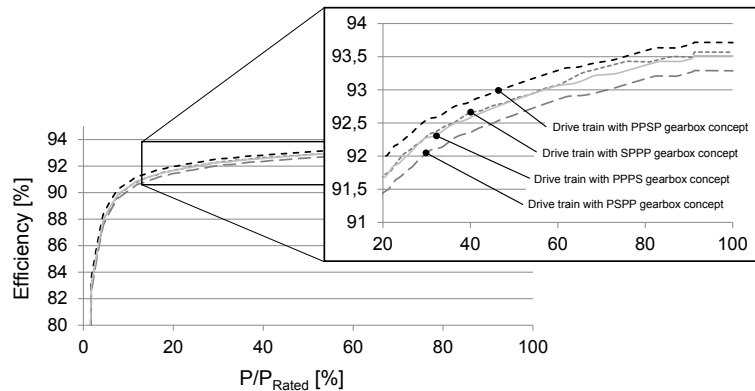


Figure 4: Results of the efficiency evaluation for different drive train configurations.

design and dimensioning. Particularly, the discrete steps between the used bearing sizes lead to different losses that influence the efficiency graphs. The simulation models for the different drive train configurations have been iteratively extended by adapting the gear and bearing parameters. Further adaptations regarding the simulation parameters are expected during the design process, which will lead to changes in the efficiency graphs.

Besides the advantages of modularity and weight, the SPPP gearbox concept also offers the greatest potential to improve the utilization capacity of the components and the increase in efficiency during partial load operation. This is due to the possible integration of switchable couplings in the gearbox, immediately after the first gear stage. In the next step of the design process, a housing including a cooling concept are developed for the SPPP concept.

## 6. Generator Topology

Three common electrical machine topologies are evaluated for their application in the proposed drive train. The evaluation is mainly based on the Esson power coefficient  $C$ , which is a parameter for the performance and

utilization of an electrical machine. The Esson power coefficient directly relates the power that can be obtained from an electrical machine to its volume and speed. It can be calculated based on the tangential force  $\sigma$ , which acts on the surface of the machines rotor [14].

The tangential force depends on the design of the machine and can therefore be used to compare different machine types.  $\sigma$  is proportional to the current distribution  $A$  and the normal component of the magnetic field induction  $B$ . The magnetic field induction is limited by the nonlinear saturation of the soft magnetic electrical sheets in the stator and rotor of the machine. The current distribution depends on the electrical utilization and thus on the cooling of the machine [14].

Table 2 shows the tangential forces and the Esson power coefficients for the considered electrical machines. Typical values of other machine parameters needed for the calculation (power factor  $\cos\varphi$ , winding factor  $\xi$  and efficiency  $\eta$ ), are given as well.

The synchronous machine with permanent magnet excitation (PMSM) offers the highest

Electrical machine	Typical values	Tangential force $\sigma$ [kN/m <sup>2</sup> ]	Esson power coefficient $C$ [kW·min/m <sup>3</sup> ]	
Squirrel cage induction machine SCIM	$A = 40,000 \text{ A/m}$ $B = 0.8 \text{ T}$	$\cos\varphi = 0.85$ $\xi = 0.95$ $\eta = 0.95$	17.36	2.86
Electrically excited synchronous machine EESM	$A = 40,000 \text{ A/m}$ $B = 1.2 \text{ T}$	$\cos\varphi = 0.90$ $\xi = 0.95$ $\eta = 0.96$	27.57	4.54
Permanent magnet synchronous machine PMSM	$A = 40,000 \text{ A/m}$ $B = 1.2 \text{ T}$	$\cos\varphi = 0.90$ $\xi = 0.95$ $\eta = 0.97$	28.15	4.63

Table 2: Tangential force and Esson power coefficient for different electrical machines (compare [14]).

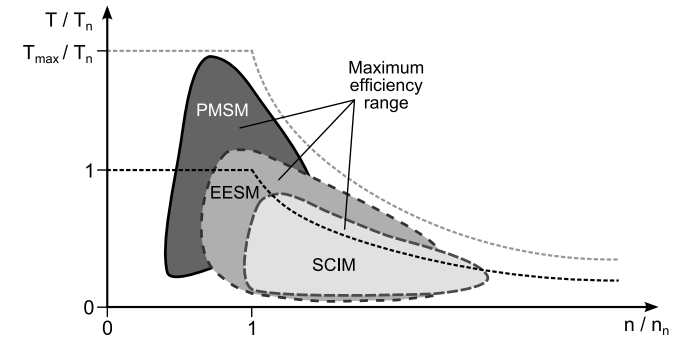


Figure 5: Exemplary efficiency ranges for different electrical machine topologies [15].

power density, when compared to the other machine types. Synchronous machines are magnetically excited by a winding on the rotor (EESM) or by permanent magnets (PMSM). These types of magnetization lead to average values of the air gap flux density of  $B = 1.2 \text{ T}$ . For the induction machine with squirrel cage rotor (SCIM) the magnetization is generated by the current in the stator winding. Air gap magnetic flux densities of  $B = 0.8 \text{ T}$  can be reached. Higher air gap flux densities would lead to an increase in magnetization effort and reduce the power factor, due to the nonlinear behavior of the stator sheet material.

Both synchronous machines have higher efficiency in the base speed range, with the PMSM being most efficient, since no copper losses occur inside the rotor due to the permanent magnet excitation. This is most advantageous for the application as a WT generator, which generally operates in the base speed range. The induction machine has the highest efficiency in the field-weakening area, as illustrated in Figure 5.

For the high-speed application of the generator further requirements have to be regarded. Especially the mechanical stress on the rotor of the machines due to centrifugal forces has to be analyzed. For the proposed application, the circumferential speed should not exceed  $100 \text{ m/s}$ , which constraints the diameter of the rotor at  $D = 0.38 \text{ m}$  (for a given speed of  $n = 5,000 \text{ rpm}$ ). The mechanical stress has local hot-spots, depending on the geometry. For the PMSM high stress occurs at the bridges around the permanent magnet slots. Another important aspect at higher speeds are the iron losses inside the electrical steel sheets, which become critical with increasing frequency and magnetic flux density [16].

A SCIM is designed for a rated power of  $P = 1 \text{ MW}$  and a rated speed of  $n = 5,000 \text{ rpm}$  based on analytical methods and considering

the values in Table 2. The resulting machine has a total volume of  $0.1116 \text{ m}^3$  (including end windings of stator winding) and a power density of  $8.96 \text{ MW/m}^3$ . With a specific price of  $16 \text{ €/kg}$  for copper and  $5 \text{ €/kg}$  for electrical sheet [1], [17], [18], the cost of the active magnetic material for one SCIM is  $4,758 \text{ €}$  (see Table 4).

The PMSM is designed with V-shaped buried magnets to minimize eddy current losses inside the magnets [16]. Table 3 lists the main parameters and Figure 6 depicts the cross section of the machine. An efficiency map is calculated for this design by means of the finite element method (FEM). A maximum efficiency of  $98.6 \%$  can be reached (see Figure 7). The resulting design has a total volume of  $0.1104 \text{ m}^3$  and thus a power density of  $9.06 \text{ MW/m}^3$  (see Table 4). To analyze the high mechanical stresses that occur in the electrical sheets of the rotor, especially in the bridges around the buried permanent magnets, a FEM calculation is performed. The geometry is too complex for an analytical consideration. The evaluation is based on the von Mises stress. The rotor geometry is optimized so that the resulting maximum value is  $419.7 \text{ MPa}$ , which is less than typical values of modern electrical sheets. Thus, the von Mises stress is below the yield strength of the material.

The cost of the total active magnetic material for one PMSM amounts to  $5,727 \text{ €}$ . A specific price for permanent magnets of  $58 \text{ €/kg}$  is assumed [1], [17], [18]. As shown in Table 4, the SCIM has a cost advantage of about  $17 \%$  over the PMSM. However, it must be considered that the power factor of the SCIM is lower compared to the PMSM (see Table 2), which means that the converter has to provide a higher apparent power. This leads to a larger size and cost of the converter.

Due to its high power density, the PMSM is chosen as generator and regarded in following simulations.

Machine parameters		
Rated power	$P_N$	1 MW
Rated voltage	$U_N$	690 V
Rated speed	$n_N$	5,000 rpm
Active length	$l_i$	480 mm
Stator		
Outer radius	$r_{S,out}$	240 mm
Rotor		
Outer radius	$r_{R,out}$	150 mm
Inner radius	$r_{R,in}$	70 mm
PM height	$h_{PM}$	10 mm
Pole pairs	$p$	3

Table 3: Parameters of the PMSM.

The vibration behavior of the developed drive train has to be evaluated, in order to make sure that no resonant frequencies are excited and to guarantee a safe and stable operation. For this purpose, a modal analysis of the PMSM with its mechanical structure (housing, shaft, bearings etc.) is performed by means of structural-dynamic simulations. Figure 8 shows that resonant frequencies of the PMSM occur above its maximum operating mechanical frequency of  $f_m = 83.33$  Hz (at 5,000 rpm). This ensures that no resonant frequency is excited by the operating speed. To rule out additional resonant

Electrical machine	SCIM	PMSM
Outer diameter	478.23 mm	480.00 mm
Total length (incl. end windings)	621.26 mm	610.00 mm
Volume	0.1116 m <sup>3</sup>	0.1104 m <sup>3</sup>
Power density	8.96 MW/m <sup>3</sup>	9.06 MW/m <sup>3</sup>
Efficiency	95 %	98 %
Active material costs	4,758 €	5,727 €

Table 4: Comparison of the SCIM and PMSM concepts.



Figure 8: First six modes of the PMSM including mechanical structure.

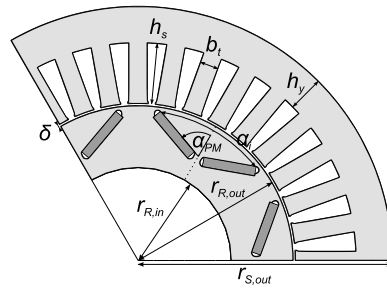


Figure 6: 120° cross section of the PMSM.

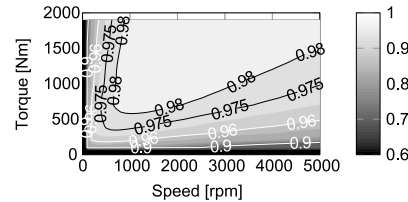


Figure 7: Efficiency map of the PMSM.

frequencies, that can have other excitation sources, further simulations are required. A vibration analysis of the entire drive train will be carried out in future works by means of multibody simulation (MBS).

## 7. Operating Strategy

A drive train concept with multiple generators offers the possibility to switch off individual generators during partial load operation, so that the remaining generators can work at their rated operating point and in their optimum efficiency range. The decoupling of total gear trains by using switchable clutches in the gearbox can offer further potential for increasing the efficiency during partial load operation.

During start-up and full load operation the operating strategy is identical compared to conventional WTs. The strategy during partial load operation has to be extended. Using six generators, the partial load operation needs to be divided into six individual operating areas. Each of these areas must be provided with both a speed control and a pitch control strategy, in order to protect the WT during short-term changes of the wind speed. The possible ranges of operation during partial load operation are dependent on the torque characteristics of the electric generators and are limited by the rated torque.

In order to meet these requirements, a generic WT controller is developed, which in a first step uses a characteristic-curve based WT analogous model. Thereby, the inertia is reduced to a single mass and the aerodynamic rotor torque and the rotor speed are calculated depending on the rotors  $c_p$ -characteristic.

The WT analogous model is loaded with wind loads that are calculated via a wind file generated using the tool TurbSim from NREL. According to the wind conditions, the pitch angle and the necessary number, torque and speed of generators are simulated by the controller.

Figure 9 depicts a simulated start-up at an average wind-speed of 14 m/s and a turbulence of 16 %. In the beginning the rotor blades are turned away from the wind and the pitch angle is 90°. The main controller initiates the start-up sequence if the wind speed is high enough for a given period of time. Then, the blades are turned into the wind with a rate of 3°/s. First, at 15s a rise of the generator speed can be noticed. This late rise is due to the WT operating

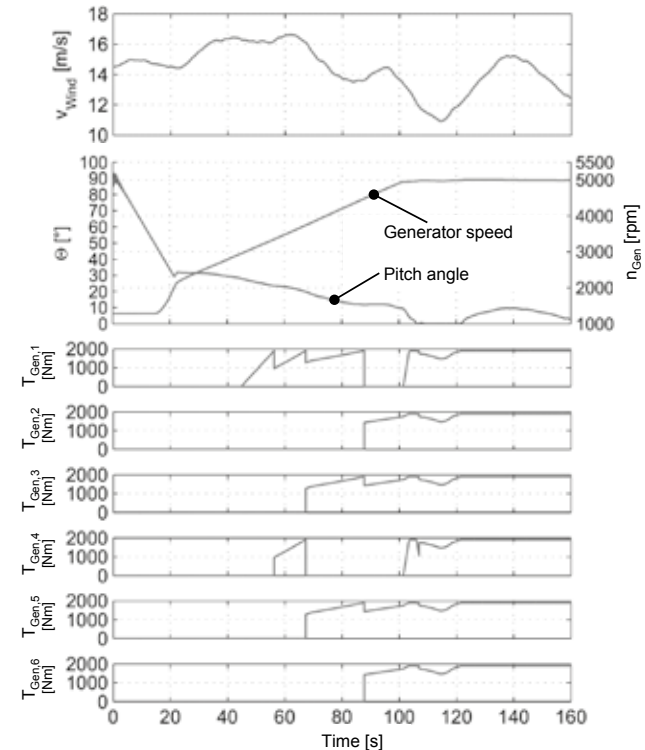


Figure 9: Simulation of the WT operating strategy during start-up with a generic controller.

point, which is still outside the  $c_p$ -characteristic of the analogous model. At 45s the switching on speed is reached and the first generator is switched on. While the rotor speed increases, the torque rises until the generator has reached rated torque. At this point the second generator is switched on and the torque is distributed symmetrically on both generators. Further generators are connected successively this way, as soon as the operating generators reach their rated torque of  $T_n = 1,900$  Nm.

In the shown start-up process of the WT the switching procedure of individual generators takes place until four generators are activated. The state of operation with five operating generators will be skipped, because the generator speed increases rapidly and torque dynamics have to be avoided. The state between 106s and 107s shows this switching procedure. The torque on the fourth generator drops to switch on to the operation mode with five generators. Before the torque can drop to 0 Nm, the torque controller activates all six generators. With increasing wind speed, full load operating range is reached (from 120s).

An idealized switching procedure; comparable to the switching procedure presented above, has been added to the efficiency calculation model in section 5 to show the potential of increasing the efficiency during partial load operation. The moments of connection or disconnection of several generators are defined by reaching a multiple of their rated torque ( $T_n = 1,900$  Nm). In the drive train model in

section 5, the gear trains which are not required, can initially also be decoupled and switched on separately together with the generators. This behavior simulates the use of a coupling after the spur gear stage and therefore after the power split in the gearbox.

The results of this efficiency simulation for different drive train configurations are shown in Figure 10. The results show a significant efficiency increase in the lower range of the partial load operation, due to the connection of individual drive trains. As soon as all generators are switched on, the efficiency characteristic is the same as in the case where no switching procedure is used. Examining the efficiency trends for the operating strategy with individual switching of generators, efficiency drops can be seen at the switching points. These result from the additional losses at low torque operating points, after an individual gear train including generator has been connected.

The greatest efficiency increase (more than 7 %) is reached for the drive train configuration with power split in the first gear stage. For this concept, three planetary stages per gear train are decoupled and thus the highest number of parts is disconnected from the power flow, when compared to the other concepts.

This efficiency increase leads to a higher electrical output power of the WT and to a higher energy yield. In low-wind regions the WT operates up to 70 % of the total operating time

at partial load. Therefore, the use of such a drive train concept with the illustrated switching procedure is particularly suitable for these locations. The WT energy output is calculated by multiplying the wind speed dependent electrical output power by the relative occurrence of the wind speed. For a low-wind site with a mean wind speed of 5.3 m/s an increase in energy yield during partial load operation of up to 1.15 % is achieved, only when using a switching procedure for individual gear trains and generators. The energy needed for the switching process is not regarded.

## 8. Conclusion

This paper describes the development of an alternative drive train configuration with six high-speed generators (rated at 1 MW and 5,000 rpm) for a 6 MW WT. Different gearbox concepts and electrical machines have been investigated, in order to determine the potential of a higher power density and an efficiency increase, as well as the advantage of a mechanical power split in the gearbox and an electrical power summation on the grid side. The SPPP gearbox configuration shows advantages regarding both weight and modularity. Efficiency simulation models for the entire drive train were created, considering a PMSM topology as a generator.

Simulation results display an efficiency increase of up to 7 % during partial load operation, provided that an operating strategy is considered, where gear trains and generators are individually connected and disconnected.

## Acknowledgement

This work was funded by the German Federal Ministry for Economic Affairs and Energy under Grant 0325642.

## References

- [1]. H. Polinder, F. F. A. van der Pijl, G.-J. de Vilder and P. J. Tavner, "Comparison of Direct-Drive and Geared Generator Concepts for Wind Turbines," *IEEE Transactions on Energy Conversion*, vol. 21, no. 3, pp. 725-733, 2006.
- [2]. S. Hoenderdaal, L. Tercero Espinoza, F. Marscheider-Weidemann and W. Graus, "Can a dysprosium shortage threaten green energy technologies?," *Energy*, vol. 49, pp. 344-355, 2013.
- [3]. T. Barthel, K. van Gelder and R. Zeichfuß, "HybridDrive 3.0 MW - Development and Testing of a New Drive Train Concept," in *Conference for Wind Power Drives*, Aachen, 2013.
- [4]. Clipper Windpower Plc, *Liberty 2.5 MW Wind Turbine*, Product Brochure, 2009.

- [5]. Winergy, "Multi Duored," 2015. [Online]. Available: <https://www.winergy-group.com/cms/website.php?id=/en/products/gear-boxes/multi-duored-gearbox.htm>. [Accessed 05 October 2015].
- [6]. E. Hau, *Wind Turbines: Fundamentals, Technologies, Applications, Economics*, London: Springer, 2013.
- [7]. G. Bywaters *et al.*, "Northern Power Systems WindPACT Drive Train Alternative Design Study Report," Technical Report, NREL, Colorado, 2005.
- [8]. Schaeffler Gruppe Industrie (Schaeffler Group Industry), *Großlagerkatalog (Large Bearings Catalogue)*, Firmenschrift (Product Brochure), 2009.
- [9]. N. E. Anderson and S. H. Loewenthal, "Spur-Gear-System Efficiency at Part and Full Load," NASA Technical Paper 1622, Technical Report 79-46, 1980.
- [10]. A. S. Terekhov, "Hydraulic losses in gearboxes with oil immersion," *Russian Engineering Journal*, vol. 55, 1975.
- [11]. D. Strasser, *Einfluss des Zahnflanken- und Zahnkopfspiels auf die Leerlaufverlustleistung von Zahnradgetrieben (Influence of Tooth Flank and Tooth Tip Backlash on the No-Load Losses of Gearboxes)*, Bochum: PhD Thesis, 2005.
- [12]. G. Niemann and H. Winter, *Maschinenelemente, Band II, Getriebe allgemein, Zahnradgetriebe - Grundlagen, Stirnradgetriebe (Machine Elements, Vol. II, Gearboxes, Gear Transmissions - Fundamentals, Spur Gears)*, Berlin: Springer, 1989.
- [13]. H. Linke, *Stirnradverzahnung, Berechnung - Werkstoffe - Fertigung (Spur Gears, Design - Materials - Manufacture)*, Munich: Hanser, 2010.
- [14]. G. Müller, K. Vogt and B. Ponick, *Berechnung elektrischer Maschinen (Design of Electrical Machines)*, Weinheim: Wiley-VCH, 2008.
- [15]. T. Finken, *Fahrzyklusgerechte Auslegung von permanentmagneterregten Synchronmaschinen für Hybrid- und Elektrofahrzeuge (Driving Cycle Based Design of Permanent Magnet Synchronous Machines for Hybrid and Electric Vehicles)*, Aachen: PhD Thesis, 2011.
- [16]. T. Finken, M. Hombitzer and K. Hameyer, "Study and Comparison of several Permanent-Magnet excited Rotor Types regarding their Applicability in Electric Vehicles," *Emobility - Electrical Power Train*, pp. 1-7, 2010.
- [17]. Argus Media, "Metal-Pages," [Online]. Available: <http://www.metal-pages.com/>. [Accessed 5 October 2015].
- [18]. London Metal Exchange (LME), "London Metal Exchange," Hong Kong Exchanges and Clearing (HKEx) Group, [Online]. Available: <http://lme.com/>. [Accessed 5 October 2015].

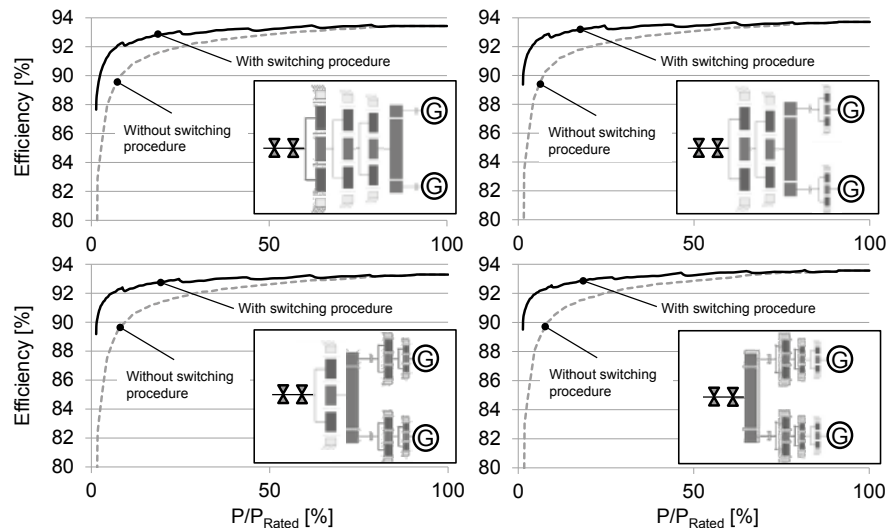


Figure 10: Efficiency characteristics without and with power split for different drive train configurations.